21. V. L. Zimont and Yu. N. Trushin, "Ignition delay in hydrocarbon fuels at high temperatures," *Fiz. Goreniya Vzryva*, **3**, No. 1, 86 (1967).
22. G. Freeman and A. N. Lefebore, "Spontaneous ignition characteristics of gaseous hydrocarbon—air mixtures," *Combust. Flame*, No. 58, 153 (1984).

FRACTAL STRUCTURE FORMATION IN EXPLOSION

A. P. Ershov and A. L. Kupershtokh

UDC 530.1+538.91+662.215.1+666.233

In the explosion of condensed explosive materials the release of free carbon is typical. The chemical reaction can proceed under conditions of diamond stability. Some results relative to the diamond phase have been described in [1, 2]; experiments performed in 1963-1965 are recalled in [3]. Note has been taken in [1-5] of the ultradispersion in diamond powders. The powder grains are conglomerates consisting of particles with characteristic dimensions of about 40 Å.

A two-stage model of particle growth in the condensed phase during an explosion [6, 7] has been introduced in the present study. By means of coagulation small compact particles are formed in the first stage, while in the second stage the particles are combined into aggregates (clusters) exhibiting a fractal structure, which is confirmed by data from small-angle x-ray scattering. The possibility of a fractal nature for aggregates in stored powders is cited in [2, 8].

In our opinion, the formation of fractal clusters must take place directly behind the detonation front, i.e., within microseconds. This leads to consequences which may be important in understanding the physics of detonation.

In an explosion free carbon is released within ~0.1 μsec, i.e., the time of the chemical reaction within the front of the detonation wave. The charactristic time t_H of hydrodynamic disintegration is expressed in units of microseconds. The quantity of carbon may be >10% of the charge mass, which corresponds to an atom concentration of $n_C \sim 10^{22}$ cm^{-3}. With such strong nonequilibrium, virtually every particle collision must lead to their merging into one another, i.e., the initial stage of particle growth must be rapid coagulation.

The Smolukhovskii theory of rapid coagulation [9] brings us to the following results. The mean particle mass (in the units of mass of the carbon atom) increases linearly over time [10]:

$$\langle m \rangle \sim K n_C t,$$

where the coagulation constant $K = 4kT/3\eta$; η is the viscosity of the detonation product. Let us note that because of the great density of the medium, particle motion, even of the smallest particles, proceeds in the diffusion Stokes regime. This serves to validate the Smolukhovskii theory for all particle sizes. In a rarefied medium such as, for example, atmospheric air, for particles small in comparison to the intrinsic Brownian mean-free path, coagulation is slightly accelerated (the free-molecular regime) [11].

We will take the temperature $T \approx 3000$ K of the detonation product (DP) and the viscosity $\eta = 10^{-2}$ poise [10^4 dynes/cm^2] on the basis of computations presented in [12] (the elementary gas-kinetic estimate from [13] yields $3 \cdot 10^{-3}$ poise). Then the product $Kn_C \approx 10^{12}$ 1/sec. Within the time $t_H \sim 1$ μsec particles consisting, on the average, of 10^6 atoms with dimensions of ~200 Å must be formed. Indeed, characteristic is a particle dimension of 40 Å, i.e., the mass is smaller by 2 orders of magnitude. At the same time, the experiment from [5] shows no relationship between particle size and t_H (proportional to the dimensions of the charge). Consequently, the growth of compact particles must be limited.

Furthermore, we will assume that two particles will combine with one another when they meet, provided that at least one of these contain atoms smaller than $m_0 = 10^3$, i.e., in terms of size <20 Å. There are a number of arguments in favor of such a condition [2], in particular, a reduction in the effective melting temperature for small particles [14]. As a result, small particles may react in the manner of liquid droplets, whereas large particles will not enter into combination. An analogous effect is achieved by the rise in fluctuations for small particles and the increase in the relative role of the surface. Of course, a realistic transition from unitary to zero probability of particle combination will not be pronounced, and the characteristic value of m_0 should be understood as a quantity chosen on the basis of its order of magnitude. The model being discussed here will therefore serve as a first approximation, and its use is justified by the imprecision with which the characteristics of the medium and of the coagulation process are known.

Let us introduce the concentration n_m for particles containing m atoms. The Smolukhovskii system of equations has the form

Novosibirsk. Translated from Fizika Goreniya i Vzryva, No. 2, pp. 111-117, March-April, 1991. Original article submitted September 5, 1990.

0010-5082/91/2702-0231$12.50 ©1991 Plenum Publishing Corporation

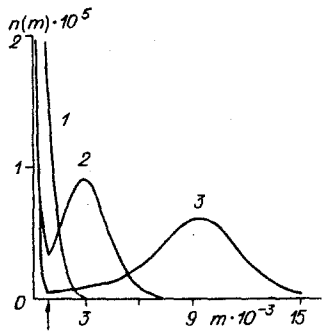

Fig. 1

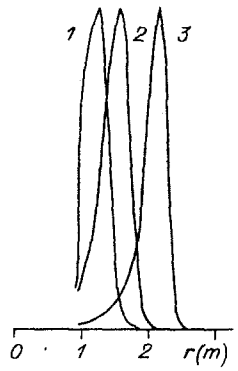

Fig. 2

Fig. 1. Distribution of concentrations through the mass with particle merging limited [curves 1-3 correspond to the dimensionless time $t_1 = m_0^{1/2} = 31.6$, $t_2 = (10m_0)^{1/2} = 100$, and $t_3 = 10m_0^{1/2} = 316$; the arrow indicates the m_0 boundary above which large-particle merging is forbidden].

Fig. 2. "Frozen-in" distribution of particles by size for various values of the reaction time t_r [curves 1-3 have been derived from distributions 1-3 in Fig. 1 and correspond to the values for the reaction times within which carbon is released: t_r = 1, 10, and 100 nsec; the boundary dimension $r(m_0)$ is taken as unity and the curves are normalized to a single amplitude].

$$\frac{dn_m}{dt} = K\left(\sum_{j=1}^{m-1}{}' F_{j,m-j}n_j n_{m-j} - 2n_m \sum_{j=1}^{\infty}{}' F_{j,m}n_j\right) + S_m.$$

The first term in the parentheses is the speed with which particles of mass m appear out of various j + (m — j) combinations, while the second term describes the reduction in the number of m particles owing to reaction with any other particle. The factor $F_{j,m} = (r_j + r_m)^2/4r_j r_m$ takes into account the difference in the dimensions r of particles with masses j and m. For identical particles we have $F_{jj} = 1$, while for particles which are different from one another there is a rather weak function of the mass ratio (for example $F_{1,10} = 1.155$). The quantity S_m describes the influx of carbon particles during the course of the chemical reaction. Assuming uniform release of single atoms during the reaction time t_r, we will write $S_1 = n_C/t_r$ and $S_i = 0$ for i > 1. The prime indicated at the summation signs denote that t least one of the colliding particles must be smaller than m_0 (the remaining terms are dropped).

Let us turn to dimensionless quantities by introducing the units of time $(t_r/Kn_C)^{1/2}$ and concentration $(n_C/Kt_r)^{1/2}$, and here, for the dimensionless concentrations and times we will retain the earlier notation. Then, until conclusion of the reaction we have

$$\frac{dn_m}{dt} = 2\left(\sum_{j=1}^{M_1} F_{j,m-j}n_j n_{m-j} - n_m \sum_{j=1}^{M_2} F_{j,m}n_j\right) + \delta_{m,1}. \tag{1}$$

Here $M_1 = \min(m/2, m_0)$; $M_2 = m_0$ for $m > m_0$, $M_2 = \infty$ for $m < m_0$; $\delta_{m,1}$ is the Kronecker delta.

The solution of the system in the absence of limitations on combination was studied analytically in [15] for $F_{j,m} = 1$ and numerically in [16]. For the dimensionless time $t \approx 5$ a distribution of $n_m \propto m^{-3/2}$ is worked out. Only the boundary at which this function is curtailed will subsequently depend on time: $m_b \sim t^2$. A gasdynamic analogy is appropriate here: the wave generated by the influx of particles is propagated along the "axis of masses" at the origin of this axis.

When m_b reaches the order of m_0, i.e., for the time $t > m_0^{1/2}$ the prohibition against combination sets in for large particles. However, small particles ($m < m_0$) continue to combine with large particles. As a result, the spectrum of the masses, although more slowly, continues to change. The qualitative behavior of the spectrum for the case in which $m >> m_0$ can be understood if we assume that m is a continuous variable. Then

$$n_{m-j} = n_m - j\frac{\partial n_m}{\partial m} + \frac{j^2}{2}\frac{\partial^2 n_m}{\partial m^2}$$

(the series expansion is effective, since $j < m_0 << m$). Moreover, we assume that $F_{j,m-j} = F_{j,m}$. As a result, we derive the simple equation

$$\frac{\partial n_m}{\partial t} + C\frac{\partial n_m}{\partial m} = \nu\frac{\partial^2 n_m}{\partial m^2},$$

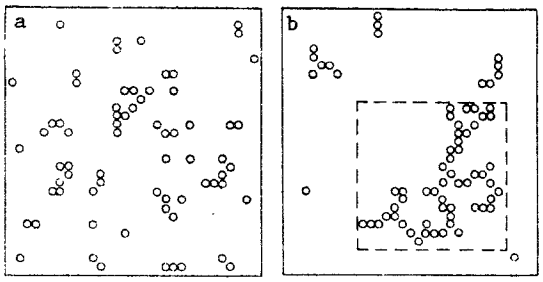

Fig. 3. Cluster—cluster association.

where $C = 2\sum_{j=1}^{m_0} jn_jF_{j,m}$, $\nu = \sum_{j=1}^{m_0} j^2n_jF_{j,m}$ depend on time through the spectrum of sizes n_j for particles and on mass through $F_{j,m}$. Both of these are weak functions, so that in first approximation we have an equation with constant factors. We should anticipate the appearance of a n(m — Ct) wave, spreading out as a consequence of the viscosity ν.

The numerical solution of system (1) demonstrates the origination at the boundary $m = m_0$ and subsequent propagation of the wave (Fig. 1). Curve 1 when $t = \sqrt{m_0}$ virtually "does not notice" the boundary $m = m_0$, while on the curves 2 and 3 ($t = \sqrt{10m_0}$ and $\sqrt{100m_0}$) concentration at the boundary drops sharply. Nevertheless, the velocity of the wave is nearly that of the value calculated from the unperturbed distribution. We note that when $t \geq \sqrt{m_0}$ the main mass is concentrated in the large particles, whereas a a large portion of the concentration is made up of small particles.

The dimensionless time for the conclusion of the reaction

$$t_* = t_r/\sqrt{t_r/Kn_C} = \sqrt{t_rKn_C}.$$

If we interrupt the reaction at the instant at which it reaches the distribution shown in Fig. 1, curves 1-3 will correspond to various reaction times: $t_r = t_e^2/Kn_C = 1$, 10, and 100 nsec for $t_e = \sqrt{m_0}$, $\sqrt{10m_0}$, and $\sqrt{100m_0}$. The true reaction time will be smaller than the gross time 0.1 μsec (for example, if the reaction involves the burning out of the hot spot). At the end of the reaction, within a time of the order $\sqrt{m_0}$ the small particles "die out" and a frozen distribution sets in, such as that shown in Fig. 2 in dependence on particle size. In all of the cases the range of sizes is quite narrow.

The assumed release of carbon in the reaction in the form of single atoms is not fundamental. In the release of larger fragments (but, of course, small in comparison to m_0) the results do not change. The "instantaneous" release of carbon ($t_r = 0$) yields a result that is close to $t_r = 1$ nsec (see Figs. 1 and 2, curves 1). Thus, limiting coagulation makes it possible to achieve a particle size nearly that of what is actually observed. Varying the parameters m_0 and t_r makes possible a more precise experimental fit. It is obvious that the "smearing" of m_0 leads to a broadening of the spectrum.

In the case of high temperatures in the zone of the detonation wave where coagulation occurs, the parameter m_0 increases. The dimensions of the compact particles will then increase slightly. Moreover, for certain explosive compositions it may be possible to achieve liquid-phase stability parameters (see, for example, [3]), and we might expect the formation of considerably larger compact particles. The imprecision of the phase diagram and of the temperature of the detonation product for the time being prevents us from indicating any explicit examples; however, it is a good idea to continue our research along these lines.

The second stage (formation of aggregates of small compact particles) begins in parallel with the conclusion of the first stage. At least, at the beginning of this process it is natural to assume that when any two clusters encounter one another, they will link up, preserving their individuality. We know [10, 17] that with such a cluster—cluster association fractal structures are formed. In this case, the cluster mass Z (the quantity of particles within the cluster) and the dimension R (in units of the diameter of a single compact particle) will be linked by the relationship

$$Z \sim R^D,$$

where D is the fractal (usually a fraction) dimension which is smaller than that of the space. Numerical simulation and experiment for the described conditions yields values of D = 1.78-2.1, i.e., with an increase in the size of the cluster its average density is reduced (the fraction of voids increases).

Figure 3 illustrates aggregation in two-dimensional space. A "box" consisting of 31 × 31 cells contains 70 particles, and these move sequentially in randomly chosen directions. The particles which are located in adjacent cells combine and then move on together. Figure 3a shows the onset of this process, as several small clusters are formed. In a later stage (Fig. 3b) we see a large cluster to which, after all is said and done, all of the remaining particles connect. Large aggregates in two-dimensional space exhibit

dimensionality of 1.44 [17] and, consequently, are markedly rarefied. At an original particle concentration of only 7% the dimension of the aggregate in Fig. 3b is of the dimensional order of the box.

Let us qualitatively examine the formation of aggregates in cluster—cluster association. The Smolukhovskii system of equations is also suitable for this process. If we neglect the polydispersion of the clusters (assuming that $F_{j,m} = 1$) and summing all of the equations in (1), for the aggregate concentration A we obtain

$$\frac{dA}{dt} = \frac{dP}{dt} - A^2,$$

where P represents the concentration of compact particles (solitary clusters). On conclusion of the reaction dP/dt = 0 and, consequently, $A \sim 1/t$. The accumulated quantity $P \sim m_0^{-1/2}$, as is clear from the above-cited distribution $n_m \sim m^{-3/2}$. The average number of particles in the cluster will then be

$$Z = P/A \sim t/\sqrt{m_0}$$

or in dimensional units $Z = t/\tau$, $\tau = \sqrt{t_r m_0/Kn_C}$.

When we take into consideration hydrodynamic expansion, the time t should be limitd to t_H, so that the maximum $Z \sim t_H/\tau \sim 100$ for $t_H = 1$ μsec, $t_r = 100$ nsec, $\tau = 10$ nsec. The cluster size $R \sim Z^{1/D} \sim Z^{1/2} \sim 10$ particle dimensions, or 300-400 Å.

The standard method of investigating fractal structures is the method of small-angle x-ray scattering (SAXS). Scattering through an angle θ corresponds to the transmitted pulse $q = 4\pi/\lambda \cdot \sin(\theta/2)$, whose reciprocal is the characteristic probe dimension. In the fractal interval of dimensions the intensity of scattered radiation $I \sim q^{-D}$ [17], which allows us to determine the scale of D. The measurements were carried out by V. N. Kolomiichuk (The Catalysis Institute, Siberian Branch, Academy of Sciences of the USSR). The radiation wavelength is 1.54 Å (CuK_α), and the range of scattering angles is $-7' < 2\theta < 7°$. The intensities measured for the "orange peel" geometry of the experiment were recalculated for "spot source" conditions. Figure 4 shows the results for two diamond powder specimens, such as were obtained in various experiments. Curve segments with a slope of nearly —4 correspond to scattering in individual particles (the Poroda regime). In the interval $5 \cdot 10^{-3} < q < 3 \cdot 10^{-2}$ 1/Å the slope indicates a fractal scale of $D \approx 1.9$, which corresponds to the cluster—cluster association. The boundaries of the fractal interval allow us to evaluate the characteristic dimensions 1/q of a particle and an aggregate (30 and 200 Å). Analogous results were obtained for mining specimens (a mixture of diamonds and graphite), taken for analysis subsequent to an explosion without chemical purification.

Another approach to the analysis of the SAXS involves an attempt to obtain the diamond particle distribution function on the basis of size [5]. It was assumed here that the scattering proceeds independently on individual spherical particles. For the distribution function f(R) we then have the integral equation

$$I(q) = \int_0^\infty f(R)\, I_R(q)\, dR,$$

where $I_R(q) = (3 \sin(qR) - qR \cos(qR))^2/q^6$ represents the intensity with which a sphere of dimension R accomplishes scattering. Such types of inverse problems, as a rule, are not stable. This is expressed in the fact that owing to the errors in the recording of the experimentally measured quantities and in approximation of the finite-sum integral large errors may arise in the unknown functions. In particular, in the problem being considered here the f(R) graphs exhibit oscillation for large R.

For a more detailed analysis of the situation, we undertook independent computation for the determination of f(R). As an example, we processed the experimental SAXS data shown in Fig. 4. We used the Phillips regularization method [18] with minimization of the functional

$$\Phi(f) = \sum_{i=1}^{n} \left(I(q_i) - \sum_{j=1}^{m} f(R_j)\, I_{R_j}(q_i)\, \Delta R_j \right)^2 + p \int_{R_1}^{R_m} \left(\frac{d^2 f}{dR^2} \right)^2 dR,$$

where n is the number of experimental points; m is the number of discretization points in the unknown function f(R); p is the regularization parameter.

The results obtained are shown in Fig. 5. Curve 1 represents the reproduced particle distribution function based on particle size. We can see that the primary peak occurs at dimensions of ≈30 Å. Despite all the attempts to vary the regularization parameter, there existed oscillations in the solution for large R, and additionally, there were negative values.

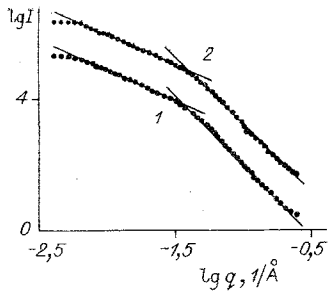

Fig. 4

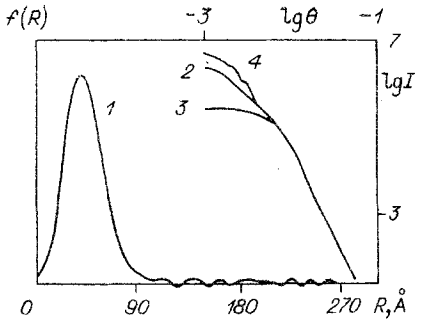

Fig. 5

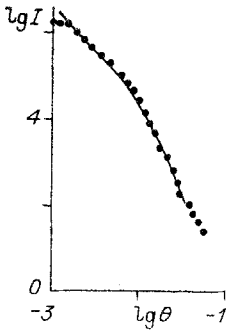

Fig. 6

Fig. 4. X-ray radiation scattering intensity, referred to a "spot source," as a function of the transmitted pulse q [the slopes of the straight lines: (—1.94 and —4.18) for the first specimen and (—1.89 and —4.10) for the second specimen].

Fig. 5. Distribution of diamond particles by size expressed as the function f(R) and the control calculations expressed as the function I(q).

Fig. 6. X-ray scattering intensity from a set of fractal clusters (the solid line represents theory, while the points represent experiment).

Based on the found distribution f(R) for control purposes we calculated the intensity I(q) (see Fig. 5, curve 2), which virtually coincides with the original experimental points. Although the oscillations in f(R) are small, their contribution to the scattering is significant. As an example, we calculated the SAXS intensity for the primary peak (R < 120 Å) and the nonnegative portion of f(R) (see Fig. 5, curves 3 and 4). For $q < 3 \cdot 10^{-2}$ 1/Å, in the place of the fractal segment ($D \approx 2$), existing in the experimental data, we observe a pronounced elevation in I(q) in the latter case, while the substance with a constant concentration of noninteracting particles enters the scattering regime in the former case.

The oscillations in f(R) can be explained as an "attempt" through the algorithm to reflect the appearance of structures in the fractal region. At the same time, in the Poroda regime (an area of scattering independent of the particles) the derived distribution function better describes the experiment than does the monodisperse (quite narrow) distribution. Apparently, a complete representation of the system is offered by a combination of these two approaches. For example, Fig. 6 shows the results from the scattering of a number of clusters with D = 2 and various sizes for the particles making up these clusters, said particles subject to the distribution in the primary peak (R < 120 Å) shown in Fig. 5. Agreement with experiment is virtually complete.

The results of the experiment and the theoretical estimates are in good agreement with the hypothesis related to the formation of fractal structures even prior to the dispersion of the detonation product. Let us indicate the consequences of these fractal structures: an aggregate of lower average density occupies the "excess" space. With a true volumetric condensed-phase fraction α_0 the "swelling" leads to $\alpha_0 \sim \alpha_0 R^{3-D} \sim \alpha_0 R$ (for $D \approx 2$). In the case of $\alpha_0 \sim 0.1$ and $R \sim 10$ we have $\alpha \sim 1$ and the clusters will consequently come into contact with one another (i.e., gelation is possible). The condition $\alpha \sim 1$ limits the dimensions of the cluster, regardless of t_H. In the disintegration of the medium (DP) the gel will tear apart in the decompression wave. Within the specimens conserved, out of the original aggregates, structures of the following microscopically observed sequences [4] collect. We should note that these processes may be burdened by phase transitions and by a change in the rheology of the medium.

Let us recall that in the work of Hayes [19] the electrical conductivity of the explosive detonation product with a high carbon content was explained by the formation of a three-dimensional grid out of graphite particles. Fractal concepts make such a picture

entirely natural. This alters the usual view of the detonation products. At least until noticeable expansion, they are not a dust-laden gas, but rather a gas-saturated porous medium.

The authors would like to express their gratitude to A. I. Lyamkin, A. M. Staver, and V. A. Molokeev for the experimental specimens; to V. N. Kolomiichuk for the SAXS measurements; to V. F. Anisichkin and to I. Yu. Mal'kov for useful discussions; to V. M. Titov for his attentiveness to this study. The research was conducted under a grant (G4-8900) from the Hydrodynamics Institute.

LITERATURE CITED

1. A. I. Lyamkin, E. A. Petrov, A. P. Ershov, et al., "Obtaining diamonds out of explosive materials," *Dokl. Akad. Nauk SSSR,* **302**, No. 3, 611-613 (1988).
2. N. Roy Greiner, D. S. Phillips, J. D. Johnson, et al., "Diamonds in detonation soot," *Nature*, **333**, 440-442 (1988).
3. K. V. Volkov, V. V. Danilenko, and V. I. Elin, "Synthesis of diamonds from the carbon in explosive detonation products," *Fiz. Goreniya Vzryva,* **26**, No. 3, 123-125 (1990).
4. A. M. Staver, N. V. Gubareva, A. I. Lyamkin, et al., "Ultradisperse diamond powders, obtained by utilizing the energy of an explosion," *Fiz. Goreniya Vzryva,* **20**, No. 5, 100-104 (1984).
5. V. M. Titov, V. F. Anisichkin, and I. Yu. Mal'kov, "Investigating the processes of synthesizing ultradisperse diamonds in detonation waves," *Fiz. Goreniya Vzryva,* **25**, No. 3, 117-126 (1989).
6. E. P. Ershov and A. L. Kupershtokh, "Formation of fractal structures in an explosion," in: Problems of Synergetics. Transactions of the Scientific-Technical Conference at Ufa, Ufa Petroleum Institute (1989).
7. A. P. Ershov and A. L. Kupershtokh, "Explosive formation of fractal structures," *Pis'ma Zh. Tekh. Fiz.,* **16**, No. 3, 42-46 (1990).
8. G. V. Sakovich, V. D. Gubarevich, F. Z. Badaev, et al., "Aggregation of diamonds obtained from explosive materials," *Dokl. Akad. Nauk SSSR,* **310**, No. 2, 402-404 (1990).
9. M. V. Smoluchowski, "Versuch einer matematishen theorie der koagulationskinetik kolloider losungen," *Zeitschrift fur Physikalishe Chemie,* **92**, 129-168 (1917).
10. B. M. Smirnov, "Fractal clusters," *Usp. Fiz. Nauk,* **49**, No. 2, 177-219 (1986).
11. S. K. Friedlander, *Smoke, Dust, and Haze: Fundamentals of Aerosol Behavior*, New York (1977).
12. M. S. Shaw and J. D. Johnson, "Carbon clustering in detonations," *J. Appl. Phys.,* **62**, No. 5, 2080-2085 (1987).
13. A. P. Ershov, "Ionization in the detonation of condensed explosive materials," *Fiz. Goreniya Vzryva,* **11**, No. 6, 928-944 (1975).
14. T. Stace, "How small is a solid?" *Nature*, **331**, 116-117 (1988).
15. J. D. Klett, "A class of solutions to the steady-state, source-enhanced, kinetic coagulation equation," *J. Atmospheric Sci.,* **32**, 380-389 (1975).
16. L. F. Mocros, J. E. Quon, and A. T. Hjelmfelt, Jr., "Coagulation of a continuously reinforced aerosol," *J. Colloid Interface Sci.,* **23**, 90-98 (1967).
17. R. Julien, "Fractal aggregates," *Usp. Fiz. Nauk*, **157**, No. 2, 339-357 (1989).
18. N. G. Preobrazhenskii and V. V. Pikalov, *Unstable Problems in the Diagnostics of Plasma* [in Russian], Nauka, Novosibirsk (1982).
19. B. Hayes, "On the electrical conductivity in detonation products," in: 4th Symp. (Int.) on Detonation, Washington (1967).